31. Knoepfel H, Spong D A *Nucl. Fusion* **19** 785 (1979)
32. Zaitsev V V, Khodachenko M L *Izv. Vyssh. Uchebn. Zaved. Radiofiz.* **40** 176 (1997)
33. Dennis B R *Lect. Not. Phys.* (2005) (in press)
34. van den Oord G H J *Astron. Astrophys.* **234** 496 (1990)
35. Lee R, Sudan R N *Phys. Fluids* **14** 1213 (1971)
36. Yokoyama T et al. *Astrophys. J.* **576** L87 (2002)
37. Bespalov P A, Trakhtengerts V Yu, in *Voprosy Teorii Plazmy* (Problems in Plasma Theory) Vol. 10 (Ed. M A Leontovich) (Moscow: Atomizdat, 1980) p. 88 [Translated into English: *Reviews of Plasma Physics* Vol. 10 (Ed. M A Leontovich) (New York: Plenum Press, 1986) p. 155]
38. Stepanov A V et al. *Publ. Astron. Soc. Jpn.* (2005) (in press)
39. Bianda M et al. *Astron. Astrophys.* **434** 1183 (2005)
40. Bespalov P A, Zaitsev V V, Stepanov A V *Astrophys. J.* **374** 369 (1991)
41. Aschwanden M J et al. *Astrophys. J.* **520** 880 (1999)
42. Rosenberg H *Astron. Astrophys.* **9** 159 (1970)
43. Zaitsev V V, Stepanov A V, in *Issledovaniya po Geomagnetizmu, Aeronomii, Fizike Solntsa* (Studies in Geomagnetism, Aeronomy and Solar Physics) Issue 37 (Moscow: Nauka, 1975) p. 3
44. Nakariakov V M, Stepanov A V *Lect. Not. Phys.* (2005) (in press)
45. Stepanov A V et al. *Pis'ma Astron. Zh.* **30** 530 (2004) [*Astron. Lett.* **30** 480 (2004)]

PACS numbers: 78.70.Bj, **98.35.–a**, **98.70.–f**
DOI: 10.1070/PU2006v049n03ABEH005969

Annihilation emission from the galactic center: the INTEGRAL observatory results

E M Churazov, R A Sunyaev, S Yu Sazonov,
M G Revnivtsev, D A Varshalovich

1. Introduction

The narrow positron annihilation line at the energy 511 keV is the brightest line in the emission spectrum of our Galaxy at energies above 10 keV. A spectral feature at energy ~ 476 keV in the radiation from the galactic center region was discovered more than 30 years ago by detectors with low energy resolution during balloon flights [1]. Soon after, observations carried out with high-resolution Ge detectors reliably identified this feature with the narrow positron annihilation line at 511 keV [2]. Later on, the annihilation emission was detected in several other experiments. Despite repeated observations, no final answer on the nature of the annihilation emission of the Galaxy has been obtained so far. This is primarily due to the existence of several principally different mechanisms for producing positrons, including:

radioactive β^+ decay of unstable isotopes, for example, ^{26}Al or ^{56}Co, produced in supernova and nova explosions;

decay of π^+ mesons arising from the interaction of cosmic rays with matter;

electron–positron pair production in high-energy photon interactions or in strong magnetic fields near compact sources — black holes or radio pulsars, and

production of positrons from dark matter particle annihilation.

Although this list is incomplete, it clearly demonstrates a great diversity of mechanisms discussed — from the commonly accepted (supernova nucleosynthesis) to the most exotic (dark matter annihilation).

Key explanations of the nature of the 511-keV line comprise: (a) determination of the space distribution of the annihilation radiation in the Galaxy and its comparison with that of potential positron sources, and (b) detailed studies of the annihilation radiation spectrum and obtaining restrictions on properties of matter in which the annihilation occurs. These are the problems that should be resolved by the INTEGRAL observatory equipped with a high-resolution Ge spectrometer.

2. Observations and data analysis

The INTEGRAL observatory is a project of the European Space Agency with the participation of Russia and the USA. The observatory was launched into a high-apogee orbit with a period of 3 days by the Proton rocket in October 2002. To investigate the annihilation emission, the SPI device [3] consisting of 19 independent high-purity Ge crystals that provide an energy resolution of about 2 keV at 511 keV was used. A tungsten mask with a thickness of 3 cm was installed at 171 cm from the detector. This mask provides modulation of the radiant flux registered by the detector. The field of view of the telescope is around 30°. In our analysis, we have made use of data obtained in the period from February to November 2003. The total observation time amounted to 3.9×10^6 s [4].

The energy scale in each observation was controlled by the location of bright background lines (^{71} Ge, 198.4 keV; ^{69}Zn, 438.6 keV; ^{69}Ge, 584.5 keV, and ^{69}Ge, 882.5 keV) seen in the spectrum taken by each detector. After such calibration, the typical amplitude of variations with time of the background line locations near 500 keV was less than 0.01 keV. The positron annihilation line is also present in the background spectrum of the SPI telescope. This line is due to positrons produced and annihilated inside detector's body and in the surrounding materials exposed to high-energy charged particles. Because the spectral line produced by the positron annihilation in the telescope material was broadened with respect to telescope intrinsic resolution, the actual energy resolution was determined from interpolation of the observed widths of two lines, 438.6 keV and 584.5 keV, symmetrically located around the 511-keV line. The energy resolution at 511 keV, determined in this way, corresponds to 2.1 keV (full width at half maximum, FWHM) for the entire data set.

Modeling the background spectrum of the telescope has required serious effort. During observations of the Galactic Center region, the background flux at 511 keV is approximately 50–100 times above the desired signal, and therefore the background model should predict it with an accuracy much better than 1%. To construct the background model, we have used observed data obtained from different regions of the celestial sphere located at angular distances of more than 30° from the center of the Galaxy. The total exposure of observations used to construct the background model was around 3.7×10^6 s. The model accounts for the background variations related to variations in the charged particle flux and the gradual accumulation of long-lived unstable isotopes inside the detector body.

3. The map of the Galaxy in the 511-keV line

Figure 1 shows the map of the surface brightness of galactic emission in the 511-keV line. In each observation, the detected 508–514-keV flux (with the model background

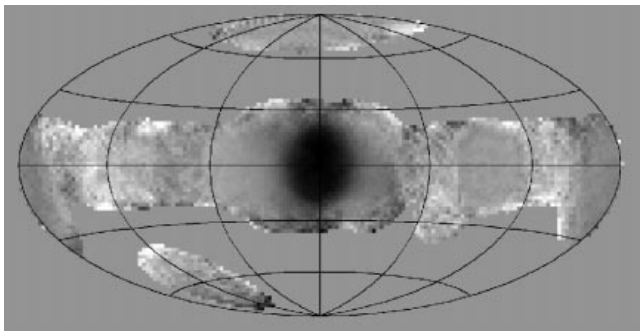

Figure 1. Distribution of galactic surface brightness in the 511-keV line. High surface brightness is shown by dark color. The map is constructed in the galactic coordinates centered at the Galactic Center. The map is strongly smoothed as it is constructed. The central spot shows that the surface brightness of annihilation emission is large in the central zone of the Galaxy, and is small in other directions.

subtracted) was distributed over the section of the celestial sphere within the telescope's field of view with a weight proportional to the effective area for 511-keV photons arriving from the given direction. Thus, the map constructed is the convolution of the true surface brightness distribution of the annihilation emission with a kernel depending on the instrumental field of view and the orientation of the telescope in each observation. On this map, only spatial scales exceeding the size of the field of view are retained, while small-scale structures are strongly suppressed. Nevertheless, this map allows the assessment of the global distribution of the annihilation emission in the Galaxy. In particular, the central region of the Galaxy (the bright spot at the map's center) is apparently a powerful source of the 511-keV line emission. The surface brightness of other regions of the Galaxy is much lower, and intensity variations seen in Fig. 1 correspond to the expected statistical noise.

Stronger restrictions on the surface brightness distribution parameters can be obtained by assuming a model brightness distribution in the Galaxy with several free parameters, and then by convolving this distribution with the instrumental response and comparing the result with direct measurements. The best values of parameters are determined by minimizing the χ^2 value:

$$\sum_i \left[\frac{AP_i - (D_i - B_i)}{\sigma_i}\right]^2 = \min\,, \qquad (1)$$

where the summation is done over all observations in which the telescope axis was pointed within 30° off the galactic center, A is the model normalization, P_i is the predicted count rate for a given detector in the i-th observation, D_i is the observed count rate in the 508 – 514-keV energy range, B_i is the predicted background count rate, and σ_i is the statistical error in the given observation. For a small number of counts in an individual observation ($N_i \leqslant 10-20$), the use of the simplest Poisson error $\sigma_i = \sqrt{N_i}$ frequently leads to the measurement and error correlation, as well as to a systematic shift in the parameter estimates [5]. To avoid this, errors were calculated from the known observation time using the mean values obtained from a large number of measurements. In the simplest model, it is assumed that the surface brightness is described by a two-dimensional Gaussian symmetrical relative to the Galactic Center. The normalization (the total flux) and width of the distribution were free model parameters. A slightly more flexible model includes an additional constant base defined as $AP_i + C$. Figure 2 depicts the total flux as a function of the Gaussian width for these two models and the dependence of $\chi^2 - \chi^2_{\min}$ [equation (1)] for the model with a constant base. The value of $\chi^2_{\min}$ equals 38,938 for 38,969 degrees of freedom (the number of individual measurements with the number of free parameters subtracted). As the signal-to-noise ratio is fairly low for individual observations, the small value of $\chi^2_{\min}$ is not a good indication of the consistency of data with the model, but rather indicates that the statistical measurement error was correctly estimated. Figure 2 implies that the best fit to observed data is achieved at a Gaussian width of around 6°. The total flux (the normalization of the Gaussian) therewith amounts to $\sim 7.6 \times 10^{-4}$ photons per s per cm^2 for the model with the base, and $\sim 10^{-3}$ photons per s per cm^2 for the model without the base. Such a difference in the radiant flux suggests a more complicated flux distribution than was assumed in these simple models. Nevertheless, the obtained value of flux reflects (to within a numerical factor on the order of unity) the total flux coming from the Galactic Center region. The precise value of this numerical coefficient depends on the assumed form of the surface brightness distribution.

Therefore, the data obtained by the INTEGRAL observatory demonstrate that the surface brightness of the central zone of the Galaxy is significantly higher than in any other direction, and the total flux from the central region reaches $\sim 10^{-3}$ photons per s per cm^2. More complex models [6, 7] for the 511-keV line surface brightness distribution, which, in particular, comprise a disk component and a central spheroidal part (bulge), lead to qualitatively similar conclusions that the radiant flux for the central component is appreciably higher than for the disk component. This conclusion is valid provided that the disk thickness is smaller than several dozen degrees.

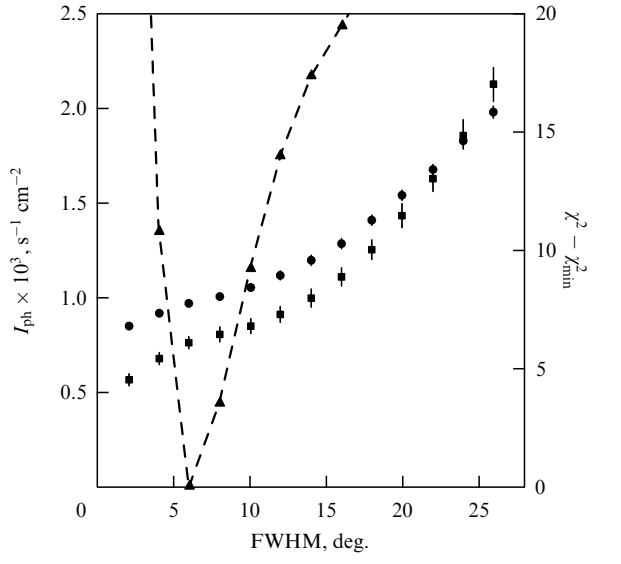

Figure 2. The flux I_{ph} in the energy range 508 – 514 keV as a function of the Gaussian width for two model surface brightness distributions: a two-dimensional Gaussian (circles), and a two-dimensional Gaussian plus a constant base (squares) . The dashed curve illustrates the dependence of the quantity $\chi - \chi^2_{\min}$ (the right axis) on the Gaussian width for the second model.

4. The spectrum of the 511-keV line emission

The data analysis in the 508 – 514-keV energy range, described in Section 3, was repeated for narrow 0.5-keV energy channels covering the range from 20 to 1000 keV. This allowed us to construct the spectrum [4] reflecting the dependence on the energy flux for a Gaussian width of 6°. This spectrum is presented in Fig. 3. The choice of the spatial model used — the Gaussian + constant (see Section 3) — is sufficiently conservative, as the inclusion of an additional free parameter decreases the statistical significance of the results, but allows the systematic noise to be suppressed. Another choice of the Gaussian width leads to changes in the spectrum normalization (see Fig. 2), but basic spectral parameters discussed in the present report are weakly dependent on the Gaussian width used. Table 1 lists parameters approximating the spectrum obtained. The spectral model includes the following components: a comparatively narrow Gaussian line (free parameters are the energy of the line center, the linewidth, and normalization), a three-photon continuum (free parameter is the normalization), and a power-law with a fixed photon index equal to 2.0. The power law was applied to take into account the hypothetical possibility that a broadband component (for example, diffuse nonthermal radiation from the interstellar medium near the galactic center) is present in the spectrum in addition to the annihilation emission. The ratio of fluxes in the first two components yields the fraction of annihilations due to positronium production:

$$F_{\rm PS} = \frac{2}{1.5 + 2.25\, F_{2\gamma}/F_{3\gamma}}\,, \qquad (2)$$

where $F_{2\gamma}$ is the line flux, and $F_{3\gamma}$ is the three-photon continuum flux. The algebraic expression (2) directly follows from the assumption that ortho- and para-positroniums are formed in the ratio 3 : 1 and give rise to 3 and 2 photons during annihilation, respectively.

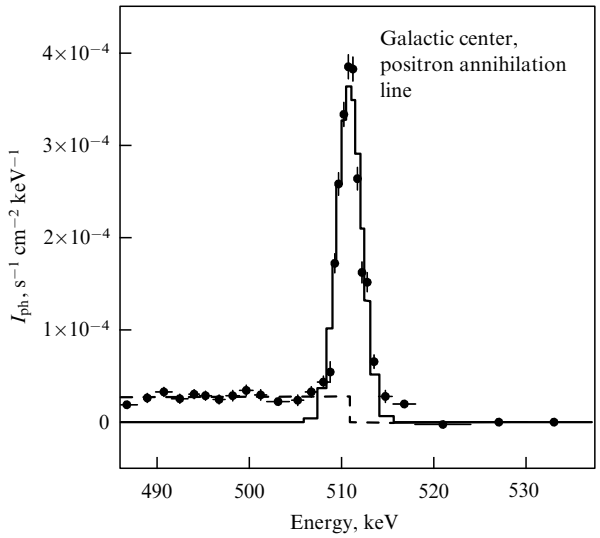

Figure 3. Annihilation emission spectrum from the central part of the Galaxy, obtained for one of the spatial model distributions of the galactic annihilation emission. Points show the three-photon decay contribution. The solid curve corresponds to the 511-keV line, while the dashed curve displays the three-photon continuum. The model curves presented have not been convolved with the instrumental energy resolution. The sharp edge of the three-photon continuum is actually smeared due to a finite resolution.

Table 1. Parameters of the spectral approximation of annihilation emission in the 450 – 550-keV range. The model includes a Gaussian line, an ortho-positronium continuum, and a power-law spectrum with a photon index equal to 2.0. Errors correspond to the 1σ confidence level for one parameter.

Parameter	Parameter value and error
E, keV	510.954 [510.88 – 511.03]
FWHM, keV	2.37 [2.12 – 2.62]
$F_{2\gamma} \times 10^4$ photons per s per cm^2	7.16 ± 0.36
$F_{3\gamma} \times 10^4$ photons per s per cm^2	26.1 ± 5.7
$F_{3\gamma}/F_{2\gamma}$	3.65 ± 0.82
$F_{\rm PS}$	0.94 ± 0.06
χ^2 (number of degrees of freedom)	192.7 (193)

5. Constraints on the interstellar medium parameters

Two measurable quantities — the linewidth and the line-to-three-photon-continuum flux ratio — allow us to put restrictions on the temperature and degree of ionization of the medium where annihilation occurs. The positrons are assumed to be born 'hot', i.e., with energies above several hundred kiloelectron-volts. Then, the positrons slow down due to Coulomb losses in an ionized plasma or atomic photoionization and excitation in a neutral gas. Ultimately, the energy of the positrons becomes comparable to the temperature in the surrounding medium — a thermalization of positrons occurs. When the energy of the positrons decreases below several hundred electron-volts, the charge exchange with neutral atoms, photorecombination, or direct annihilation with free or bound electrons become effective (see, for example, Ref. [8]). In the analysis below we have considered a pure hydrogen gas without dust. To evaluate ionization, excitation, and charge exchange processes, we have used theoretical predictions by Kernoghan [9], which well fit with observations. For photorecombination and direct annihilation on free electrons, approximations from Ref. [10] have been adopted. The direct annihilation on bound electrons has been evaluated using approximations from Ref. [11]. For positrons slowing down during ionization of hydrogen atoms, it is necessary to specify the energy distribution of electrons in the final state. To this end we have made use of the final energy distribution obtained in the first Born approximation, and the normalization has been fixed to a value from Ref. [9]. For positrons slowing down by interacting with free electrons, we applied an analytical approximation [12] obtained for the energy loss by electrons. In the calculations we have assumed that during charge exchange and photorecombination ortho- and para-positroniums are produced according to their statistical weights, i.e., in the 3 : 1 ratio.

To trace the energy evolution of positrons and the formation of the annihilation emission spectra with due regard for all above processes, a Monte Carlo method has been applied. The emission spectrum produced by thermalized positrons with the Maxwellian energy distribution has been calculated separately. Estimates show that deviations from the Maxwellian distribution due to charge exchange of positrons with neutral atoms can be important at a plasma temperature of around 6000 K and a very low degree of ionization of less than 10^{-3}. For other combinations of the

temperature and degree of ionization, deviations from the Maxwellian distribution are insignificant.

The annihilation line is predicted to have a form deviating from an ideal Gaussian and often shows the presence of both a broad and a narrow component. In that case, the linewidth traditionally defined as a 'full width at half maximum' is more sensitive to the narrow component, even if this component comprises a small fraction of the radiation. To avoid this, an effective linewidth has been calculated — the energy interval comprising 76% of the total line flux.

Results of the calculations are shown in Fig. 4, where each curve corresponds to a given temperature of the medium. The degree of ionization in the medium changes along the curves. It is easily seen that the curves presented in Fig. 4 form two families.

The first family of the curves corresponds to a gas with a temperature below ~ 6000 K. In a cold and neural medium, around 94% of positrons annihilate prior to the thermalization. The other 6% go below the positronium production threshold (6.8 eV) and then annihilate on bound electrons. The effective linewidth resulted from the positron annihilation with the positronium production is 5.3 keV. The annihilation on bound electrons yields an effective width of about 1.7 keV [13] due to the finite width of the velocity distribution of electrons bound in a hydrogen atom. The effective width (the sum of the broad and narrow components) of the line eventually formed is ~ 4.6 keV. If the degree of ionization in the medium exceeds $\sim 10^{-3}$, Coulomb losses become effective, i.e., the fraction of positrons that form positronium atoms prior to the thermalization decreases. For positrons with energies below 6.8 eV, the most important are three processes: photorecombination with free electrons, and annihilation on both free and bound electrons. At the degree of ionization on the order of 10^{-2} and temperatures of about 1000 K, the annihilation on bound electrons decreases the fraction of positronium to 80–90%. If the degree of ionization is more than several percent, only photorecombination and annihilation on free electrons are significant, and both the fraction of positroniums and linewidth converge to the values as expected in a fully ionized plasma.

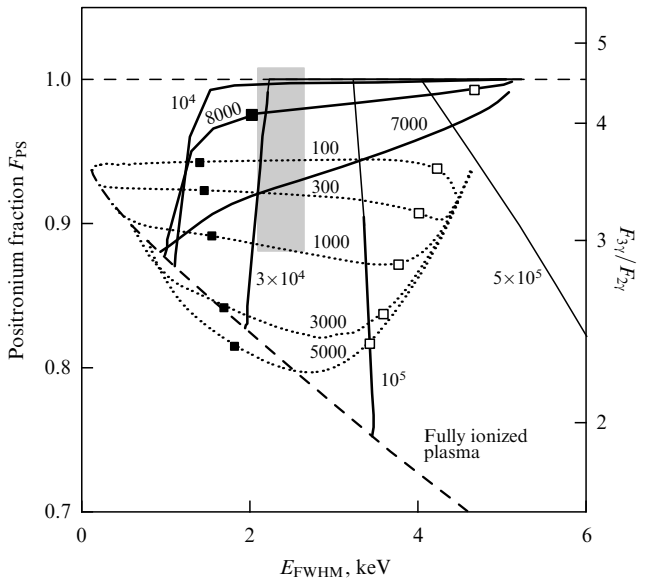

Figure 4. Effective width of the 511-keV line and annihilation fraction originating from the positronium production for different temperatures and degrees of ionization of the medium. The gray rectangle corresponds to parameter values compatible with the INTEGRAL observatory data. Theoretical curves are subdivided into two groups: low-temperature ($T < 5000$ K, dotted curves), and high-temperature ($T > 7000$ K, solid curves). The temperature is fixed for each curve (as shown in the figure), and the degree of ionization changes along the curve from 0 to 1. For low-temperature curves (and for the curve at $T = 8000$ K), the degree of ionization equal to 0.01 is marked with open squares, and the degree of ionization amounting up to 0.1 with full squares. The dashed curve is the fraction of the annihilation events due to the positronium production vs. the linewidth in a fully ionized medium.

The second family of curves corresponds to temperatures above 7000 K. At such temperatures, thermalized positrons can produce positroniums in charge exchange reactions with hydrogen atoms. This process dominates over photorecombination and direct annihilation if the plasma is not highly ionized. Here, the fraction of positronium turns out to be very close to unity. Only for a significant degree of plasma ionization (on the order of 6–10% at $T = 8000$ K, and more at higher temperatures) does the annihilation on free electrons become important, and the positronium fraction starts decreasing with increasing degree of ionization (the almost vertical portions of the curves in Fig. 4).

The calculations illustrated in Fig. 4 have been performed for different combinations of temperatures and degrees of gas ionization, without regard to the viability of these combinations in real astrophysical conditions. For comparison, restrictions on the effective linewidth and positronium fraction as inferred from the INTEGRAL observations are shown in Fig. 4 by the gray rectangle. Clearly, two solutions are possible in terms of the one-phase medium: low-temperature ($T < 1000$ K), and high-temperature ($7000 < T < 4 \times 10^4$ K). Now we shall discuss the astrophysical aspect of these solutions.

According to the standard model for the interstellar medium [14, 15], there are several principal phases in the Galaxy: hot ($T > 10^5$ K), warm ($T \sim 8000$ K), and cold ($T < 100$ K).

It follows from Fig. 4 that a hot ($T > 10^5$ K) ionized medium cannot provide the dominant contribution to the observed annihilation emission spectrum. Indeed, the width of the line originated in such a medium is too large, and the positronium fraction is too low. The positronium fraction can be formally increased by decreasing the degree of gas ionization, but it is unlikely that in astrophysical conditions the degree of ionization can be made notably lower than in the purely collisional ionization equilibrium. A restriction on the contribution from a very hot ($T > 10^6$ K) fully ionized plasma can be obtained by adding a broad line to the model spectrum and finding the maximal line amplitude that would not contradict the observed spectrum within statistical errors. For example, the expected linewidth at $T = 10^6$ K equals ~ 11 keV [16], and such a line contribution is below 17% at the 90% confidence level. Assuming that the remaining photons ($< 83\%$) in the line are due to positronium annihilation and taking into account that at this temperature the direct annihilation and photorecombination rates are almost equal, we can conclude that less than 8% of the total positronium annihilations occur in a medium with temperature $T = 10^6$ K. Note that timescales for positron slowing down and annihilation in the interstellar medium depend both on the initial positron energy and on the medium properties (mainly on its density). The admissible time interval is fairly broad. For example, the mean time prior to annihilation at an initial positron energy of 0.5–1 MeV varies

from 10 thousand to several hundred million years when passing from the cold phase to the hot phase. This means that positrons in the hot phase live sufficiently long, thus having time: (a) to leave the Galaxy or (b) to enter a denser phase and then annihilate. Consequently, a small fraction of annihilations in the hot medium is not by itself proof that positrons have not been produced in the hot medium.

A similar conclusion would also hold for a cold ($T < 10^3$ K) neutral medium. In this case, the expected positronium fraction is in agreement with observations, but the expected linewidth of about 4.5 keV is too large. It is possible to reduce the linewidth by assuming a degree of ionization significantly higher than 10^{-2}. However, such an ionization degree for molecular and cold HI clouds is significantly higher than the typical values, which renders this solution improbable.

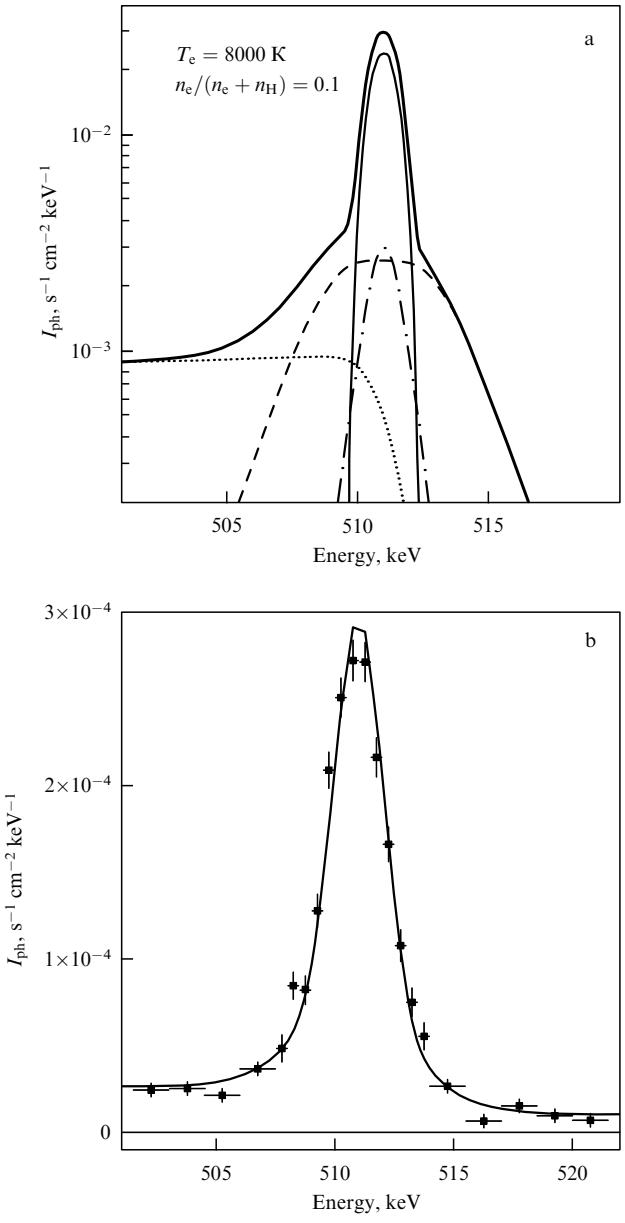

Figure 5. (a) Expected spectrum of the annihilation emission from a medium with temperature 8000 K and degree of ionization equal to 0.1. The dotted curve exhibits the contribution from a three-photon continuum; the dashed curve represents the annihilation line formed prior to thermalization of positrons; the thin solid curve corresponds to annihilation caused by production of para-positroniums after thermalizaiton, and the dot-and-dash line marks direct annihilation of thermalized positrons. The thick solid curve displays the complete annihilation emission spectrum. (b) Comparison of the model spectrum shown in figure (a) and convolved with instrumental energy resolution and the spectrum observed.

On the other hand, the degree of ionization in the warm ($T \sim 8000-10{,}000$ K) phase of the interstellar medium can vary from less than 0.1 to more than 0.8. Such a phase offers the possibility to explain the observed annihilation linewidths and positronium fractions in the spectrum. At temperatures 8000 – 10,000 K, the required degree of ionization amounts to a few percent. At a temperature of around 20,000 K, the necessary degree of ionization equals ~ 0.4. At temperatures above 30,000 K, plasma is virtually completely ionized, even if ionization by electron impact dominates. In typical astrophysical conditions, it is safe to assume that the degree of plasma ionization does not decrease below the value expected from collisional ionization by electrons. Possible photoionization additionally increases the ionization degree. Thus, the 'allowed' degree of ionization ranges from the collisional ionization value to unity. The corresponding portions of the curves in Fig. 4 are marked with the bold line.

Hence, Fig. 4 implies that the warm phase of the interstellar medium in the single-phase model provides the best fit with the spectrum observed. This conclusion is qualitatively consistent with the results [8] obtained from an analysis of earlier observations of annihilation emission. The detailed shape of the spectrum predicted by the annihilation model in a gas with temperature 8000 K and degree of ionization of 0.1 is demonstrated in Fig. 5a. The comparison of the model and observed spectra is shown in Fig. 5b.

It should be emphasized that although the single-phase model can reproduce observations quite well, more sophisticated models including annihilation in several phases [4] cannot be ruled out. The degree of phase ionization plays here a significant role. For example, the observations can be explained by assuming a presence of mixture of the cold neutral phase with a warm ionized phase in a 1:1 ratio. See papers [4, 17] for a more detailed analysis of this subject.

6. Discussion and conclusions

Observations made by INTEGRAL have provided the most precise current spectral measurements of the annihilation emission from positrons in the Galactic Center region.

The surface brightness of annihilation radiation is high in the central parts of the Galaxy (5 – 10 degrees in size), and is low in other parts. The flux from the central region amounts to $\sim 10^{-3}$ photons per s per cm^2. The uncertainty in this value is almost entirely related to that in the proposed surface brightness distribution. Assuming a distance of 8.5 kpc to the annihilation region and taking into account that the fraction of annihilations via positronium production is close to unity, we find that the observed flux corresponds to $\sim 2 \times 10^{43}$ annihilations of positrons per s. The corresponding luminosity is equal to $L_{e^+} \sim 1.6 \times 10^{37}$ erg s^{-1} (the number of positron annihilations times the positron rest energy). This puts serious energy restrictions on the positron production mechanism. For the initial positron Lorentz factor γ, the minimal expenditure of power is γL_{e^+}. If positrons originate from more energetic (or more massive) particles, the minimal power required to produce the necessary number of positrons

can be estimated as

$$\frac{E_0}{m_e c^2} L_{e^+} ,$$

where E_0 is the initial particle energy. For example, if positrons are produced by cosmic rays (via π^+-meson formation), the minimal expenditure of power equals $\approx 3 \times 273 \times L_{e^+} \approx 10^{40}$ erg s^{-1}. Here, we have taken into account that π^- and π^0 mesons are produced simultaneously with π^+ mesons. Decay of π^0 mesons must give rise to gamma emission at energies of 50 – 100 MeV with a luminosity on the order of 3×10^{39} erg s^{-1}. All these estimates, of course, have been obtained by assuming the stationarity of the annihilation emission.

An analysis of data gathered in the first series of observations indicates that the contribution from the disk component is smaller than the radiant flux from the central part of the Galaxy [6, 7]. The luminosity ratio is a model-dependent quantity strongly depending on the assumed properties of individual components, for example, on the disk component thickness.

The center of the line coincides with the rest energy of electrons (positrons) with high accuracy:

$$\frac{E}{m_e c^2} = 0.99991 \pm 0.00015 .$$

Therefore, the mean line-of-sight velocity of the medium with reference to the Earth is no more than ~ 44 km s^{-1}. Observations of the annihilation linewidth also allow us to impose restrictions on the characteristic velocity of chaotic motions in the medium. The intrinsic linewidth in a medium at rest depends on the temperature and degree of its ionization (see Fig. 4) and can be sufficiently small ($\sim 1 – 1.5$ keV). Taking this into account, a conservative upper bound on the spread in the line-of-sight velocity amounts to ~ 800 km s^{-1}.

The combination of the observed linewidth (2.37 ± 0.25 keV) and positronium fraction ($F_{PS} = 0.96 \pm 0.04$) can be explained by annihilation in a 'warm' phase of the interstellar medium with a characteristic temperature of around 8000 K and degree of its ionization on the order of 0.1. Annihilation in a single-phase cold ($T \leqslant 10^3$ K) or hot ($T \geqslant 10^5$ K) medium is inconsistent with the measurement data. However, a combination comprising several phases with different temperatures and degrees of ionization cannot also be excluded. The limit on the annihilation fraction in a very hot ($T \geqslant 10^6$ K) phase is below 8%.

The characteristics of the annihilation emission given above evidence against models of the positron origin in type II supernovae and massive stars, since such objects are found exclusively in the disk of the Galaxy and not in its bulge. Likewise (and from the energy consideration), a hypothesis for the production of positrons by interactions of cosmic rays with matter seems improbable. The INTEGRAL observatory data are more consistent with positron sources populating the Galactic bulge, in particular, with type Ia supernovae, low-mass binaries, or dark matter annihilation. Each of these mechanisms has its own advantages and shortcomings. One of the most important goals of continuing INTEGRAL observations is to impose more stringent constraints on the surface brightness distribution and spectral shape variations in the annihilation emission along and across the galactic plane. This will allow us to significantly narrow the class of physical processes mainly responsible for the production of positrons in the Galaxy.

References

1. Johnson W N (III), Harnden F R (Jr), Haymes R C *Astrophys. J.* **172** L1 (1972)
2. Leventhal M, MacCallum C J, Stang P D *Astrophys. J.* **225** L11 (1978)
3. Vedrenne G et al. *Astron. Astrophys.* **411** L63 (2003)
4. Churazov E et al. *Mon. Not. R. Astron. Soc.* **357** 1377 (2005)
5. Churazov E et al. *Astrophys. J.* **471** 673 (1996)
6. Teegarden B J et al. *Astrophys. J.* **621** 296 (2005)
7. Knödlseder J et al. *Astron. Astrophys.* **441** 513 (2005)
8. Bussard R W, Ramaty R, Drachman R J *Astrophys. J.* **228** 928 (1979)
9. Kernoghan A A et al. *J. Phys. B: At. Mol. Opt. Phys.* **29** 2089 (1996)
10. Gould R J *Astrophys. J.* **344** 232 (1989)
11. Bhatia A K, Drachman R J, Temkin A *Phys. Rev. A* **16** 1719 (1977)
12. Swartz W E, Nisbet J S, Green A E S *J. Geophys. Res.* **76** 8425 (1971)
13. Iwata K, Greaves R G, Surko C M *Phys. Rev. A* **55** 3586 (1997)
14. McKee C F, Ostriker J P *Astrophys. J.* **218** 148 (1977)
15. Kaplan S A, Pikel'ner S B *Fizika Mezhzvezdnoi Sredy* (Physics of Interstellar Medium) (Moscow: Nauka, 1979)
16. Crannell C J et al. *Astrophys. J.* **210** 582 (1976)
17. Jean P et al. *Astron. Astrophys.* **445** 579 (2006)

PACS numbers: **97.80.–d**, **98.70.–f**, 98.70.Qy
DOI: 10.1070/PU2006v049n03ABEH005970

Ultraluminous X-ray sources in galaxies — microquasars or intermediate mass black holes

S N Fabrika, P K Abolmasov, S V Karpov, O N Sholukhova, K K Ghosh

1. New class of X-ray sources

Ultraluminous X-ray sources (ULXs) in external galaxies were singled out in astrophysics as a new class of objects in 2000. Very bright X-ray sources had been discovered in galaxies earlier [1]. However, only after NASA's CHANDRA X-ray Observatory observations with a spatial resolution of $\approx 1''$ did it become clear that they constitute a new class of objects. These objects are not active galactic nuclei and not background quasars . In our report we briefly describe intriguing properties of these objects, basic models proposed for ULXs, and ideas that could help in understanding the nature of ULXs from analysis by observational methods. The last, in particular, includes studies of gaseous nebulae surrounding these objects, carried out on the 6-meter telescope of the Special Astrophysical Observatory (SAO) of RAS, as well as predictions of the specific X-ray spectra of ULXs.

ULXs are distinguished by their huge X-ray luminosities of $10^{39} – 10^{42}$ egr s^{-1} in the 0.5 – 100 keV energy range. In our Galaxy, the maximum observed luminosities from accreting black holes in close binaries amount to $\sim 10^{38}$ erg s^{-1} in 'persistent' emission (i.e., not at the peak of an outburst). In this case, measured masses of the black holes fall within the range 4 – 15 solar masses. The total X-ray luminosity of a galaxy like our own or M31 ranges $(0.5 – 1) \times 10^{40}$ erg s^{-1} (2 – 20 keV). The critical luminosity of an accreting black